Non-damaging Retinal Phototherapy: Dynamic Range of Heat Shock Protein Expression

Christopher Sramek,[1,2] *Mark Mackanos,*[2,3] *Ryan Spitler,*[3] *Loh-Shan Leung,*[4] *Hiroyuki Nomoto,*[4] *Christopher H. Contag,*[3] *and Daniel Palanker*[1,4]

Purpose. Subthreshold retinal phototherapy demonstrated clinical efficacy for the treatment of diabetic macular edema without visible signs of retinal damage. To assess the range of cellular responses to sublethal hyperthermia, expression of the gene encoding a 70 kDa heat shock protein (HSP70) was evaluated after laser irradiation using a transgenic reporter mouse.

Methods. One hundred millisecond, 532 nm laser exposures with 400 μm beam diameter were applied to the retina surrounding the optic nerve in 32 mice. Transcription from the HSP70 promoter was assessed relative to the control eye using a bioluminescence assay at 7 hours after laser application. The retinal pigmented epithelium (RPE) viability threshold was determined with a fluorescence assay. A computational model was developed to estimate temperature and the extent of cell damage.

Results. A significant increase in HSP70 transcription was found at exposures over 20 mW, half the threshold power for RPE cell death. Computational modeling estimated peak temperature $T = 49$°C at HSP70 expression threshold. At RPE viability threshold, $T = 57$°C. Similar temperatures and damage indices were calculated for clinical subvisible retinal treatment parameters.

Conclusions. Beneficial effects of laser therapy have been previously shown to extend beyond those resulting from destruction of tissue. One hundred millisecond laser exposures at approximately half the threshold power of RPE damage induced transcription of HSP70, an indication of cellular response to sublethal thermal stress. A computational model of retinal hyperthermia can guide further optimization of laser parameters for nondamaging phototherapy. (*Invest Ophthalmol Vis Sci.* 2011;52:1780–1787) DOI:10.1167/iovs.10-5917

Laser photocoagulation is a standard therapy for numerous retinal conditions, including age-related macular degeneration (AMD), diabetic retinopathy, and idiopathic central serous choroidopathy (ICSC). Absorbed by the retinal pigment epithelium (RPE) and pigmented choroid, laser energy (typically 532 nm wavelength) is converted into heat, diffusing into the retina and choroid. Laser power in photocoagulation is typically titrated to a visible clinical effect (graying or whitening of the retina), which corresponds to damage to the photoreceptors and, at higher settings, to the inner retina.[1] Although clinically effective, retinal photocoagulation frequently leads to unwanted secondary effects, including scotomata and the disruption of retinal anatomy through scarring.

One approach toward retinal phototherapy that avoids permanent damage is selective treatment of retinal pigment epithelium (SRT). In SRT, microsecond laser pulses confine damage to the RPE layer, sparing photoreceptors and the inner retina.[2] Subsequent RPE proliferation and migration restores continuity of the RPE layer.[3] Preliminary reports on SRT treatment have shown it to be clinically effective in applications to ICSC and diabetic macular edema (DME).[4–8]

Another approach to nondamaging retinal treatment is transpupillary thermotherapy (TTT). TTT involves long exposures (typically 60 seconds) of a large spot (1.2–3 mm) at low irradiance (roughly 10 W/cm^2), using a near-infrared (NIR, 810 nm) laser.[9–11] A few pilot studies have shown TTT to decrease or slow the progression of exudation and choroidal neovascularization in AMD.[12,13] However, clinical use of TTT for retinal vascular disease has been limited because of questions about its efficacy and reports of occasional retinal damage,[14,15] though it remains commonly used for treatment of choroidal melanoma.[16,17]

In addition to the long exposures of large spots used in TTT, shorter bursts of NIR radiation (810 nm) with small spot sizes (100–200 μm) have also been applied for nondamaging retinal phototherapy. This subthreshold micropulse phototherapy has recently been shown to be clinically effective in the treatment of DME and proliferative diabetic retinopathy.[18–23] Using bursts of micropulses, laser energy was applied with no visible lesions and no fluorescein leakage, as observed acutely and in subsequent clinical exams. Beneficial effects of the treatment on neovascularization and macular edema have been recorded in clinical exams and by retinal thickness measurements with OCT.[21]

The underlying mechanism of micropulse and TTT treatments is assumed to be retinal tissue hyperthermia below the threshold of cell death, although the details of this interaction remain unclear.[6,7,19–21] The underlying pathophysiology that leads to a number of retinal disorders includes inflammation and hypoxia, resulting in apoptosis or an induction of angiogenic factors such as vascular endothelial growth factor (VEGF) or inflammatory cytokines that stimulate neovascularization or vascular permeability.[24–26] Laser photocoagulation in the treatment of proliferative retinopathies is believed to decrease secretion of factors such as VEGF by destroying regions of ischemic retinal tissue. However, a method to increase the cellular capacity for repair and response to hypoxic or inflammatory stress, rather than destroy tissue as in conventional laser treatments, may be highly beneficial.

From the [1]Hansen Experimental Physics Laboratory, and the Departments of [3]Pediatrics and [4]Ophthalmology, Stanford University, Stanford, California.

[2]These authors contributed equally to this work.

Supported in part by the Air Force Office of Scientific Research, Stanford Program in Military Photomedicine.

Submitted for publication May 20, 2010; revised August 9 and September 7, 2010; accepted October 4, 2010.

Disclosure: **C. Sramek**, None; **M. Mackanos**, None; **R. Spitler**, None; **L.-S. Leung**, None; **H. Nomoto**, None; **C.H. Contag**, None; **D. Palanker**, OptiMedica Inc. (C, P)

Corresponding author: Christopher Sramek, Hansen Experimental Physics Laboratory, Stanford University, 452 Lomita Mall, Room 140, Stanford, CA 94305; csramek@stanford.edu.

Heat shock proteins (HSPs) are a group of ubiquitous, well-described proteins expressed in response to cellular stress. Acting as chaperone proteins, HSPs can assist in the refolding of denatured proteins.[27–30] These chaperones have also been demonstrated to inhibit inappropriate protein aggregation while trafficking target proteins to the proper organelles for either degradation or repair.[28,29] In addition, HSPs interact with and stabilize the cytoskeleton, maintaining cellular structure. Though found at low levels at baseline, HSPs are highly inducible. The 70 kDa heat shock protein (HSP70) in particular is known to be expressed in conditions of thermal, ischemic, and oxidative stress and is believed to be a significant component in conferring thermotolerance to heated tissue.[27,29] Ischemic insult to the rat spinal cord and brain leads to expression of the protein as early as 6 hours, even in the apparent absence of injury.[31]

Moreover, HSPs have activity against apoptotic pathways and inflammation. Multiple studies demonstrate that HSPs interfere with both caspase-dependent and caspase-independent apoptotic cascades in various tissue types, including, brain, spinal cord, and retinal ganglion cells.[31–33] HSP70 upregulates the anti-apoptotic protein Bcl-2 and may also prevent mitochondrial cytochrome c release. In addition, HSP70 prevents formation of the complex central to caspase-dependent apoptosis, the apoptosome, while also inhibiting activation of caspase-3. HSP70 also interferes with the caspase-independent apoptosis-inducing factor.[30,32–34] The role of HSP as an anti-inflammatory mediator is not well understood, although it appears to reduce the presence of inflammatory mediators such as TNF-α, possibly through interaction with NFκB (a nuclear transcription factor for multiple genes associated with inflammation) and its inhibitor, IκB.[33]

HSP70 expression in response to laser exposure has been demonstrated in the rabbit choroid and retina,[35,36] as well as in rodent choroid, retina, optic nerve head, and lens.[32,34,37,38] Careful application of laser to induce heat shock protein expression may serve a protective role, activating cellular response, and slowing or preventing apoptotic and inflammatory pathways that lead to cellular damage. To confirm any therapeutic benefit and determine the therapeutic range, it is first necessary to elaborate the threshold at which the protein is expressed, as well as the threshold at which cellular damage or death occurs. In this study, we use a well-described transgenic reporter mouse[39–42] to determine the laser exposure limits above which HSP70 is expressed, as well as the energy at which cellular death occurs, quantifying the window in which nondamaging laser could be effective.

Methods

Photocoagulation System

The laser system (PASCAL; OptiMedica Inc., Santa Clara, CA) has been previously described in detail.[43,44] Briefly, it provides 532 nm optical radiation from a diode-pumped, continuous-wave, frequency-doubled Nd:YAG laser coupled into a scanning system integrated with a slit lamp. The laser beam with a flat-top profile is projected onto the retina with variable magnification, providing a variety of spot sizes. A graphic user interface is used to control laser parameters, including the spot size, laser power, and pulse duration. Once the treatment parameters are appropriately selected, a foot pedal is used to activate the laser.

Animal Model

The transgenic HSP70-L2G reporter mouse has been described previously.[41] This mouse line is an albino mouse (strain FVB) in which the promoter from the murine HSP70A1 gene was used to express a fusion reporter gene comprising the coding sequences for a modified firefly luciferase and green fluorescent protein.[42] Homozygous albino HSP70-luciferase mice were crossed with C57BL/6 mice to create pigmented hemizygous transgenic mice for the purpose of more closely mimicking the pigmented human retina, while preserving one copy of the reporter gene as an indicator of thermal stress. Pigmented female mice hemizygous for the HSP70-L2G transgene were used in these experiments. Mice were used at approximately postnatal day 60, in accordance with the Association for Research in Vision and Ophthalmology Statement Regarding the Use of Animals in Ophthalmic and Vision Research, after approval from the Stanford University Animal Institutional Review Board. Mice were anesthetized with avertin (250 mg/kg) administered intraperitoneally 5 minutes before the procedure. Pupillary dilation was achieved with one drop each of tropicamide 1% and phenylephrine hydrochloride 2.5% administered to the right eye of each mouse.

Laser Application

A glass coverslip was used as a contact lens to focus the laser onto the retina. Exposures of 100 ms in duration with an aerial spot size of 400 μm were applied in a circular pattern around the optic nerve, between the retinal vessels. The RPE damage threshold was first determined using a propidium iodide fluorescence assay. Laser powers from 15 to 120 mW were applied to a total of 10 animals (20 eyes) in these experiments. After the RPE damage threshold was identified (40 mW), the induced bioluminescence was studied at laser power levels below the damage threshold, using increments of 5 mW: 15, 20, 25, 30, 35, and 40 mW. Ten exposures of 100 ms with an aerial spot size of 400 μm and the same power level were applied to the right eye of each mouse around the optic nerve. Three to five eyes for each power level were used in this set of measurements, 22 animals in total. Approximately 7 hours post-laser irradiation, the mice were euthanized and both eyes enucleated $<$10 minutes later.

RPE Viability: Propidium Iodide Fluorescence Assay

For the viability assay, each globe was cut equatorially, and the anterior segment and vitreous humor were removed. The neural retina was carefully peeled off to expose the RPE while preventing RPE adhesion to the retina. Samples of the posterior segment were placed in a Petri dish and stained with a standard membrane permeability assay based on propidium iodide (PI) fluorescent dye (Sigma-Aldrich, St. Louis, MO).[45–47] PI is a normally cell-impermeant molecule, which undergoes a 40-fold enhancement of fluorescence on binding to nucleic acids. PI fluorescence of the cell indicates abnormal permeability of the cell membrane or even disintegration of the membrane and nucleus.[48,49] Staining took place no more than 20 minutes after enucleation. Cell viability was assessed based on fluorescence images taken with a digital camera 20 minutes after staining, when fluorescence reached its maximum level. Images were evaluated using a software package (ImageJ, v.1.37; developed by Wayne Rasband, National Institutes of Health, Bethesda, MD; available at http://rsb.info.nih.gov/ij/index.html.).[50] The diameter of the damaged zone was defined as the geometric mean of the vertical and horizontal lesion diameters.

HSP70 Expression: Bioluminescence Assay

The retinas of the right eyes were treated at power levels varying from 15 to 40 mW, and the left eye was left untreated. Mouse eyes were enucleated at 7 hours post-laser irradiation, corresponding to maximum HSP70 bioluminescence,[42] as established in previous experiments with the HSP70-L2G reporter mouse.[41,51] Individual eyes were each placed into 1.5 mL polypropylene microcentrifuge tubes (Denville Scientific, Metuchen, NJ) and weighed. Each tube was then placed on ice, and 100 μL of 1$\times$ lysis buffer (Promega Corp., Madison, WI) was added for every 20 mg of tissue. The tissues were incubated in lysis buffer on ice for 10 minutes before grinding with a pestle in 1.5 mL polypropylene microcentrifuge tubes (Denville Scientific). One hundred microliters of luciferase assay solution (Promega Corp.) and 20 μL of the homogenized eye tissue in lysis buffer were combined in a 75 mL

tissue culture tube and resuspended (by pipette). A total of five replicates were generated for each eye, and the luciferase activity was measured in each sample using a luminometer (Berthold Corp., Pforzheim, Germany). The bioluminescent signal was acquired using a 20 second integration time.

For imaging of the luminescent spots in the retina, albino HSP70-L2G mice were injected intraperitoneally with luciferin IP at a dose of 150 mg/kg 7 hours post-laser treatment. The mice were euthanatized, and the eyes were enucleated 10 minutes after injection. The anterior segment, lens, and vitreous body were removed from the eye. The retina, RPE, choroid, and sclera were immediately placed and flattened onto a fluorodish with a cover glass bottom (World Precision Instruments, Sarasota, FL). Tissues were covered with a solution consisting of luciferin at 30 mg/mL and ATP. Images of the posterior pole were acquired using the LV200 bioluminescent imaging system (Olympus Corporation, Tokyo) equipped with a Hamamatsu EM CCD camera. Image acquisition was performed with 10× and 20× objectives using 5-minute exposures and analyzed (Metamorph Software; Molecular Devices, Sunnyvale, CA).

Statistical Analysis

The ratio of the luminescence signal from the treated and control (untreated) eyes was averaged for each treatment power. The difference between the treated/control ratio and unity was analyzed using a ratio *t*-test at each treatment power. Results were expressed as the mean treated/control ratio with 95% confidence intervals. Statistical significance was determined at a level of $P < 0.05$.

Finite-Element Computational Model

A finite-element model of retinal heating and coagulation[52] constructed with a computational package (COMSOL Multiphysics 3.5)[53] was used to estimate temperature rise at the RPE for laser powers between 10 and 150 mW. This model, developed to estimate lesion size in rabbit, approximated the retina as a series of homogeneous absorbing layers and coupled an axisymmetric heat conduction model with a cellular damage model.[54]

Although the layer absorption coefficients and Arrhenius parameters are estimated in the literature for rabbit,[52,55] similar values were unavailable for mouse, despite prevalent use of the animal in ocular laser injury studies (Muniz A, et al. *IOVS* 2009;50:ARVO E-abstract 4467).[56–58] The rabbit model included a highly absorbing pigmented choroidal layer 20 μm below the choriocapillaris,[55] which is not present in mice. This layer was omitted, and the entire thickness of the choroid was reduced to 23 μm to match thicknesses reported in literature.[59] Thickness of the neural retina, RPE, and sclera were assumed to be 220, 4, and 200 μm, respectively, matching the mouse anatomy. Differences exist in chorio-retinal pigmentation and blood perfusion between the holangiotic rodent and merangiotic rabbit retinas. However, the impact of convective cooling is negligible for subsecond duration pulses.[60] The RPE is primarily responsible in determining peak retinal temperature at 532 nm, with limited variation in fractional absorption (roughly 40–70%) across species.[55,61,62]

To assess the retinal irradiance, the retinal beam size was calculated, taking into account the expected demagnification in the mouse eye covered with a flat coverslip. Optical specifications of the mouse eye (including curvature radii of each surface, refractive indices, and surface separation distances) have been taken from the literature.[63] The addition of a coverslip and goniosol gel in front of the cornea decreased the refractive power of the mouse eye from 569 to 469 D, resulting in a magnification factor at the RPE of ×0.39. Thus, a retinal irradiance distribution with a FWHM diameter of 156 μm (90–10% falloff of 14 μm) was used in the computational model.

Laser attenuation due to small-angle scattering in the anterior segment was a significant aspect of previous retinal photocoagulation models[52,55] and laser transmittance through the eye has been measured to be between 40% and 90% in rabbits.[52,64–66] This factor has not been measured in mouse and was left as a free parameter in the current model, adjusted to fit the size of the resulting damage zone in RPE. With these modifications, temperature rise at the RPE was calculated for a 100 ms exposure at powers between 10 and 150 mW.

For pulse durations exceeding 50 μs, thermal denaturation of tissue has been shown to be the primary retinal damage mechanism.[55,67] In this regime the damage can be described with first-order reaction kinetics (Arrhenius law) parameterized by an activation energy, corresponding to the denaturation of a single critical component, and assuming an absence of cellular repair.[54] An integral of the exponential temperature-dependent reaction rate, the Arrhenius integral (Ω), quantifies the decrease in concentration of this critical component. The criterion for cell viability is then determined as a maximum tolerable decrease in concentration of the critical component; the Arrhenius integral is generally normalized to unity at this threshold. From the calculated temperature time courses for 100 ms exposures at the RPE, the Arrhenius integral was computed, and the size of the RPE damage zone was estimated as the radius where the Arrhenius integral $\Omega = 1$.[52]

For comparison with the clinical subthreshold laser therapy, a computational model of 810 nm laser heating of the human retina was constructed in COMSOL to estimate temperature and the extent of cell damage. This computational model was similar to the homogeneous absorption mouse model described above, with layer thicknesses and absorption and scattering coefficients adjusted for human retina and choroid.[68,69]

Laser parameters currently used in the subthreshold treatment of diabetic macular edema were implemented in the model: wavelength, 810 nm; burst duration, 300 ms; duty cycle, 5%; micropulse repetition rate, 500 Hz[19,21]; and laser power, 950 mW (Jeff Luttrull, private communication, 2010). With a 125 μm aerial beam diameter and a contact lens (Ocular Mainster Standard; Ocular Instruments, Bellevue, WA), the retinal diameter was assumed to be 131 μm (×1.05 magnification).[70] For comparison, retinal temperature and the corresponding Arrhenius values were computed for a continuous wave laser exposure of the same average power.

Results

RPE Viability Threshold and Computational Model

As a function of laser power, ophthalmoscopic visibility of the lesions varied from invisible at 30 mW and below, to barely visible at 40 mW, light at 50 mW, moderate at 70 mW, and intense at 90 mW. A representative image from the mouse RPE viability threshold dataset is shown in Figure 1A. Regions of stained RPE cells are clearly visible, along with the retina adherent to the optic nerve head. Lesion diameter plotted as a function of laser power is shown in Figure 2. Diameter appears to increase linearly with power above 50 mW, a trend that has been reported previously for ophthalmoscopically and histologically measured lesion widths.[1,52] Similarly, such a trend was also supported by both Arrhenius and fixed-temperature models of retinal damage.[52,71] The threshold power for RPE damage with the cell viability assay was 40 mW, as no lesion was observed at lower powers.

Lesion widths at the RPE predicted by the computational model are shown as a solid line in Figure 2. Ocular transmittance of 0.54 was found to provide the best fit to the measured data, accurately demonstrating the observed increase in lesion diameter with power. The inferred ocular transmittance completes the model and allows for the estimation of retinal temperature at both the cell viability and the HSP70 expression thresholds.

HSP70 Expression and Tissue Temperature

Because of low contrast of the fundus in pigmented mice, Figure 1B demonstrates bioluminescence in an albino transgenic HSP70-L2G reporter mouse for illustration purposes.

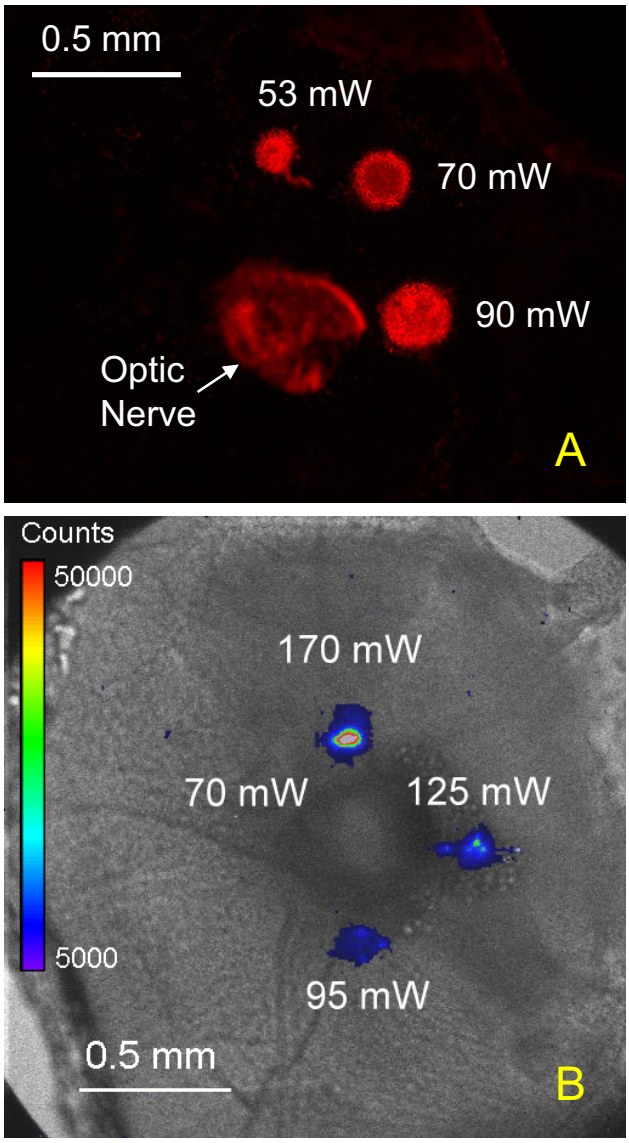

FIGURE 1. (**A**) Propidium iodide staining of mouse RPE flat-mount. Laser powers of 53, 70, and 90 mW produced visible staining, but 30 and 40 mW exposures did not. Retina adherent to the optic disc is also visible. (**B**) Bioluminescent micrograph illustrating HSP70 expression in the albino mouse retina. Applied laser power is indicated next to each lesion.

Bioluminescent signal is overlaid on the fundus photo in false color encoding light intensity. Laser power is indicated next to each treatment spot. As can be seen in this image, bioluminescent signal is localized to laser lesions. Since albino mice lack melanin, the laser light is absorbed primarily by blood, and therefore retinal heating requires significantly higher power than in pigmented mouse.

The bioluminescence signals from the pigmented mice were recorded and averaged from five samples prepared from each eye. The ratio of the averaged signal of the treated eye to that of a control eye in the same animal was then calculated for each animal. The mean value of these ratios for each power level is shown in Figure 3. The ratio is very close to unity at 15 mW and starts increasing at 20 mW, becoming statistically significant ($P < 0.01$) at 25 mW. It keeps increasing with increasing power up to the RPE damage threshold at 40 mW. It is expected to continue increasing further because larger tissue volume becomes affected at higher power levels, but

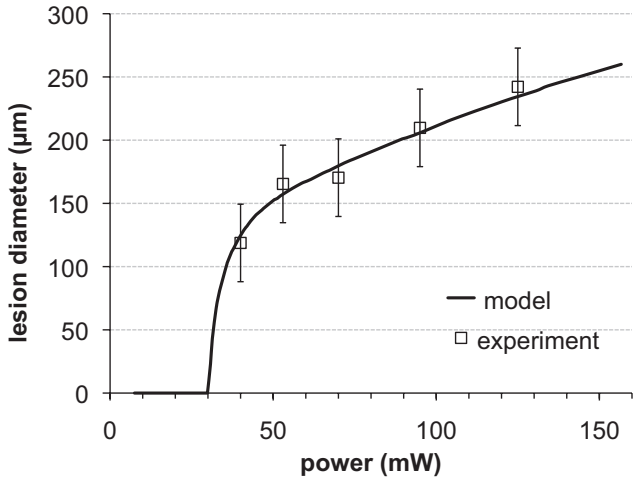

FIGURE 2. Measured diameter of RPE lesions as a function of corneal laser power (*symbols*), with estimates from the computational model (solid line). Error bar width corresponds to the pooled SD of the lesion diameters.

this study was focused only on the energy settings below the cellular toxicity level.

Calculated radial temperature profiles at the end of a 100 ms exposure at 20 mW and 40 mW are shown in Figure 4A. The peak temperature for HSP expression, 49°C, is significantly lower than that for cell death, 62°C. The corresponding peak Arrhenius values at the center of the beam are 0.08 and 6.2, respectively. The width of the damage zone (Arrhenius values $\Omega > 1$) is shown by an arrow in Figure 4B and corresponds to a radius of 60 μm.

Retinal Hyperthermia in Clinical Applications to DME

The computed traces of temperature at the RPE in the center of the beam during micropulse laser treatment are shown in Figure 5. The temperature produced by the micropulse laser oscillates around the trace corresponding to a continuous laser, with the rise time equal to 0.1 ms micropulse duration and repetition period of 2 ms. It reaches a maximum of 52°C,

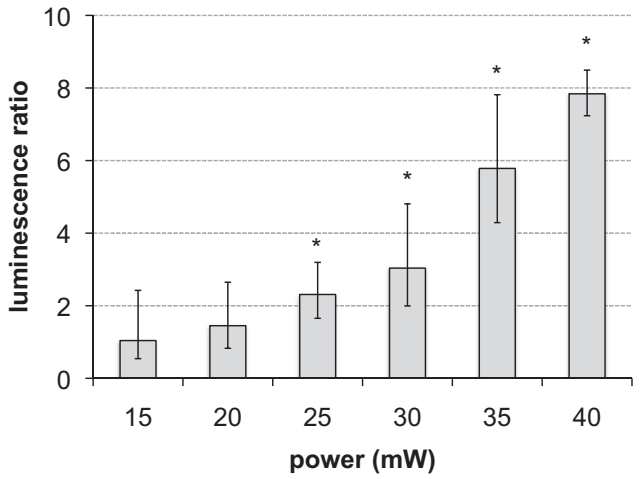

FIGURE 3. Mean ratio of the treated to control eye bioluminescence as a function of laser power, with 95% confidence intervals. *Asterisk* indicates statistical significance ($P < 0.05$). The ratio becomes significantly greater than unity ($P < 0.01$) at 25 mW and continues to increase up to the RPE damage threshold (40 mW).

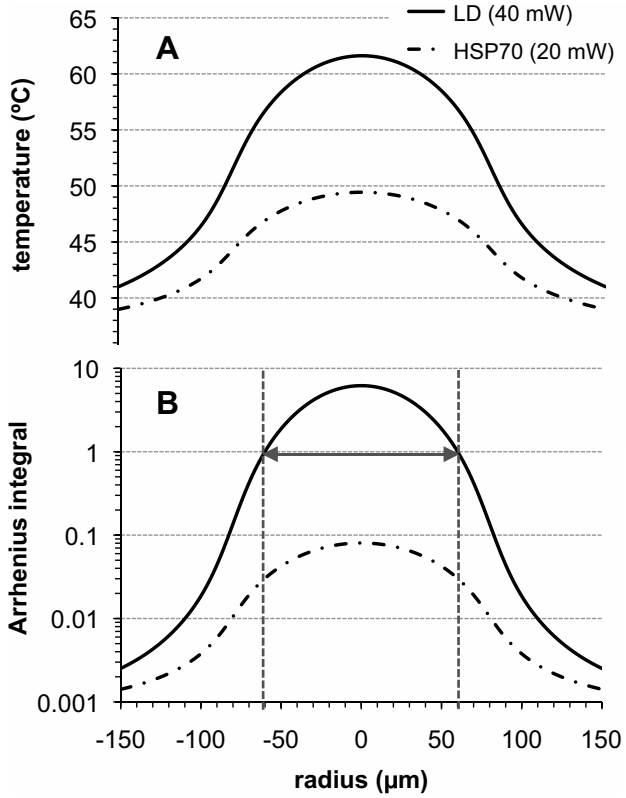

FIGURE 4. (A) Computed temperature profiles at the top of the RPE layer for live/dead (LD, 40 mW) and HSP70 expression thresholds (20 mW). (B) Corresponding Arrhenius integral for the computed temperature traces. Width of the RPE damage zone ($\Omega = 1$) is indicated. At HSP70 expression threshold, the peak value of the Arrhenius integral is approximately 10 times below the damage threshold.

whereas with the continuous laser, the temperature approaches 46°C by the end of the 300 ms pulse. Total pulse energy for both lasers at the cornea was 14.25 mJ. Corresponding Arrhenius axial profiles, shown in Figure 6, exhibit very similar values in the choroid and in the neural retina, with a pulsed laser having higher value (by approximately 20%) in the RPE.

DISCUSSION

The 40 mW RPE viability threshold elaborated above corresponds to a peak radiant exposure of 2.8 J/cm^2. A similar order of magnitude value has been previously reported for 100 ms exposures in rabbit in vivo (2.0 J/cm^2)[52] with a smaller but comparable beam size of 132 μm. Computed peak temperature at the boundary ($\Omega = 1$ radius) of the 40 mW lesion was 57°C. Previous measurements of cellular hyperthermia during prolonged exposures (>1 second) estimated cell viability threshold temperatures in the range 40–55°C.[72,73]

Increase of HSP70 expression in response to hyperthermia was previously measured after relatively long exposures (1 second or longer). In nonretinal tissue, the threshold temperatures have generally been slightly above physiologic levels (42–44°C).[74,75] The measured and computed retinal temperatures during 60-second duration TTT, associated with subsequent HSP70 expression in the choroid,[35,36] have been on the order of 47°C.[76,77] The calculated RPE temperature for 0.1-second exposures in the present study is higher, 49°C. Although the uncertainty in ocular transmittance and model absorption parameters limit the accuracy of temperature determination in the model, the agreement between predicted and measured lesion diameters gives some confidence that the combination of assumed irradiance and Arrhenius values describe the lesion formation appropriately. Since a quantitative relationship between the HSP activation and tissue hyperthermia is not well established, we did not attempt to estimate the strength of the bioluminescence signal in the model.

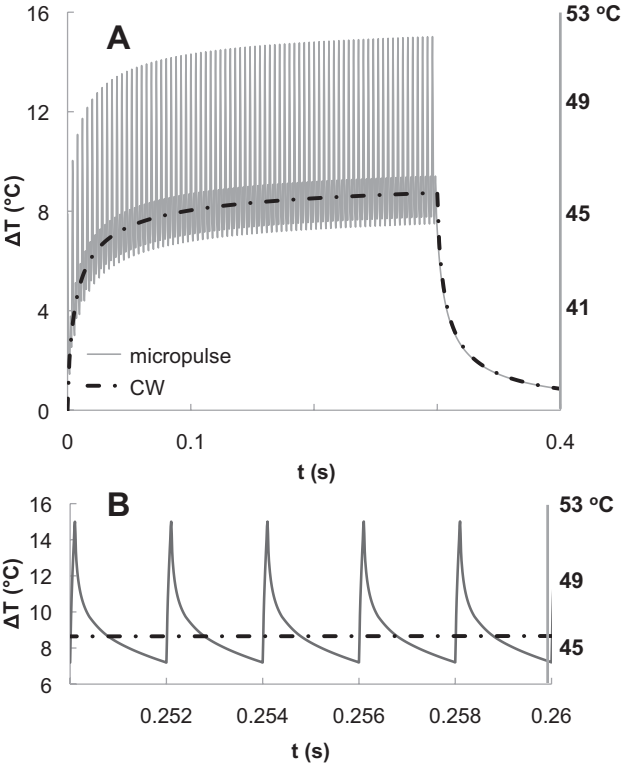

FIGURE 5. Computational results for clinical parameters. (A) Central RPE temperature rise for micropulse (500 Hz, 5% duty cycle) and continuous wave irradiation with 300 ms, 14.25 mJ exposures. (B) Five micropulse cycles illustrating heating and cooling dynamics.

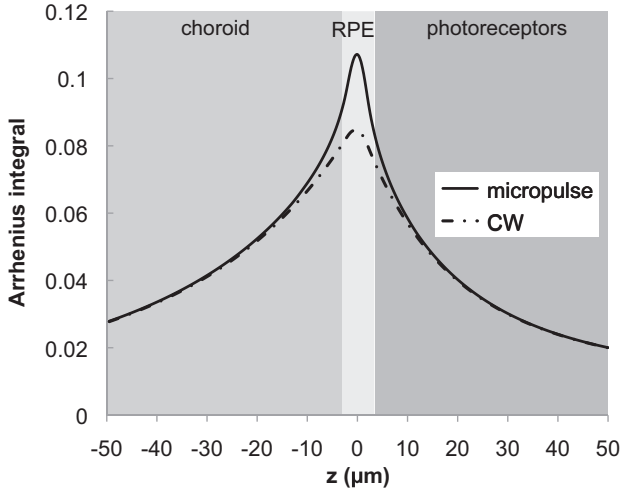

FIGURE 6. Axial profile of Arrhenius integral for micropulse and continuous wave exposures in human retina. Modest selectivity is illustrated by the higher value at the RPE, but values in the photoreceptor layer and choroid are equivalent. Peak values are comparable to those estimated at HSP70 expression threshold in the mouse model.

Several interesting observations can be made regarding the modeling of clinical laser settings. The peak Arrhenius value computed for the micropulsed laser, 0.11, is similar to the peak value estimated at HSP70 expression threshold in mice (0.08), as shown in Figure 4B (20 mW graph). This result may be an indication that the expression of HSP is an appropriate measure for assessment of tissue response to hyperthermia. Figure 6 demonstrates that Arrhenius values in the photoreceptor layer and in the choroid rapidly decrease with distance from the RPE, and thus these layers are less likely to elicit a response to laser irradiation under these conditions. The exponential dependence of critical component concentration on the Arrhenius integral[54] implies that small variations in this quantity can lead to significant differences in tissue effects. However, for the small values of the Arrhenius integral shown in Figure 6, the 20% difference in peak Arrhenius integral for micropulse and continuous wave lasers of the same average power corresponds only to a 3% difference in critical component concentration, indicating that their clinical effects are likely to be similar. This prediction should be verified in a clinical trial.

Although the estimated Arrhenius values in the models are comparable, there are important limitations to extrapolating the rodent model to the clinical situation. The Arrhenius integral is strongly dependent on temperature. Small variations in RPE pigmentation, ocular transmittance, and focusing would lead to different values. Applying model parameters across species is another concern, as Arrhenius activation energies may differ for human retinal cells. The agreement between measured and calculated lesion widths in the rodent model using the same activation energy as in rabbit[52] supports the use of this parameter across species. This assumption would benefit from a similar validation in human patients using, for example, clinical lesion width data from high-resolution optical coherence tomography. Despite the existing limitations, the computational model provides a useful theoretical context for clinical observations.

We assessed an upper limit of the thermal effect in tissues with variable pigmentation by doubling the absorption coefficients in RPE and choroid, since macular RPE pigmentation varies by no more than a factor of 2.[78] With this modification to the model, the peak Arrhenius value for a continuous laser reached 1.55, whereas for a micropulse laser it reached 4.02, indicating that a few RPE cells in the center of the laser may become damaged. Since the damage of a few cells is unlikely to be visible with a slit lamp, or with fluorescein angiography, such lesions likely will still be considered invisible. These estimates support the clinical observations with micropulse laser treatment that the described parameters, while clinically effective, do not exhibit visible signs of retinal damage.[18]

In addition, the titration procedure used in one of the clinical studies[22] matches our observations: The laser power is first titrated for producing minimally visible burns, and then the treatment is administered at half of that power.[22] Our measurements indeed corroborate that HSP70 expression begins at approximately half of the laser power required for producing RPE damage, which is slightly below the threshold for ophthalmoscopic visibility of the lesion in the millisecond range of pulse durations.[52] At such power levels retinal damage can be avoided, while biological response is elicited from the treated tissue.

The therapeutic range of nondamaging hyperthermia, defined as the ratio between the thresholds for RPE damage and HSP70 expression, measured in this work for 100 ms pulses, was found to be larger than previous estimates obtained with longer exposures and larger spot sizes. Studies by Desmettre et al.[35,36] investigated 15-to-60-second TTT in rabbit, demonstrating a factor of roughly 1.5 between visible coagulation and immunohistochemically detectable hyperexpression of HSP70 in the choroid. Treatment with shorter durations and smaller spot sizes may have the advantage of a wider therapeutic range due to more localized heating of the RPE and choroid and higher temperatures required for thermal coagulation at shorter pulse durations. The duration, spot size, and wavelength dependence of nondamaging retinal treatment require further examination.

A recent observation of VEGF and pigment epithelium derived factor upregulation in RPE organ culture after laser irradiation below the damage threshold provides further evidence of the possibility of nondamaging laser therapy (Miura Y, et al. *IOVS* 2010;51:ARVO E-Abstract 469). An accurate computational model of retinal response to nondamaging laser treatment may help in further optimizing the laser parameters to maximize the treatment selectivity and safety, that is, the range between the desirable clinical response and irreversible cellular damage.

Acknowledgments

The authors thank the Olympus Corporation for the LV200 bioluminescent imaging system and technical assistance.

References

1. Jain A, Blumenkranz MS, Paulus Y, et al. Effect of pulse duration on size and character of the lesion in retinal photocoagulation. *Arch Ophthalmol.* 2008;126:78–85.
2. Framme C, Walter A, Prahs P, et al. Structural changes of the retina after conventional laser photocoagulation and selective retina treatment (SRT) in spectral domain OCT. *Curr Eye Res.* 2009;34:568–579.
3. Roider J, Brinkmann R, Wirbelauer C, Laqua H, Birngruber R. Retinal sparing by selective retinal pigment epithelial photocoagulation. *Arch Ophthalmol.* 1999;117:1028–1034.
4. Elsner H, Pörksen E, Klatt C, et al. Selective retina therapy in patients with central serous chorioretinopathy. *Graefes Arch Clin Exp Ophthalmol.* 2006;244:1638–1645.
5. Framme C, Brinkmann R, Birngruber R, Roider J. Autofluorescence imaging after selective RPE laser treatment in macular diseases and clinical outcome: a pilot study. *Br J Ophthalmol.* 2002;86:1099–1106.
6. Framme C, Walter A, Prahs P, Theisen-Kunde D, Brinkmann R. Comparison of threshold irradiances and online dosimetry for selective retina treatment (SRT) in patients treated with 200 nanoseconds and 1.7 microseconds laser pulses. *Lasers Surg Med.* 2008;40:616–624.
7. Prahs P, Walter A, Regler R, et al. Selective retina therapy (SRT) in patients with geographic atrophy due to age-related macular degeneration. *Graefes Arch Clin Exp Ophthalmol.* 2009.
8. Roider J, Brinkmann R, Wirbelauer C, Laqua H, Birngruber R. Subthreshold (retinal pigment epithelium) photocoagulation in macular diseases: a pilot study. *Br J Ophthalmol.* 2000;84:40–47.
9. Oosterhuis JA, Journee-de Korver HG, Kakebeeke-Kemme HM, Bleeker JC. Transpupillary thermotherapy in choroidal melanomas. *Arch Ophthalmol.* 1995;113:315–321.
10. Reichel E, Berrocal AM, Ip M, et al. Transpupillary thermotherapy of occult subfoveal choroidal neovascularization in patients with age-related macular degeneration. *Ophthalmology.* 1999;106:1908–1914.
11. Mainster MA, Reichel E. Transpupillary thermotherapy for age-related macular degeneration: principles and techniques. *Semin Ophthalmol.* 2001;16:55–59.
12. Ahuja RM, Benner JD, Schwartz JC, Butler JW, Steidl SM. Efficacy of transpupillary thermotherapy (TTT) in the treatment of occult subfoveal choroidal neovascularization in age-related macular degeneration. *Semin Ophthalmol.* 2001;16:81–85.
13. Newsom RS, McAlister JC, Saeed M, McHugh JD. Transpupillary thermotherapy (TTT) for the treatment of choroidal neovascularisation. *Br J Ophthalmol.* 2001;85:173–178.
14. Mason JO, 3rd, Colagross CC, Feist RM, et al. Risk factors for severe vision loss immediately after transpupillary thermotherapy for oc-

cult subfoveal choroidal neovascularization. *Ophthalmic Surg Lasers Imaging.* 2008;39:460–465.
15. Roider J. Is there sufficient evidence to support transpupillary thermotherapy for age-related macular degeneration? *Vitreo-Retinal Surg.* 2005:67–72.
16. Parrozzani R, Boccassini B, De Belvis V, Radin PP, Midena E. Long-term outcome of transpupillary thermotherapy as primary treatment of selected choroidal melanoma. *Acta Ophthalmol.* 2008.
17. Aaberg TM Jr., Bergstrom CS, Hickner ZJ, Lynn MJ. Long-term results of primary transpupillary thermal therapy for the treatment of choroidal malignant melanoma. *Br J Ophthalmol.* 2008;92:741–746.
18. Figueira J, Khan J, Nunes S, et al. Prospective randomised controlled trial comparing sub-threshold micropulse diode laser photocoagulation and conventional green laser for clinically significant diabetic macular oedema. *Br J Ophthalmol.* 2009;93:1341–1344.
19. Luttrull JK, Musch DC, Mainster MA. Subthreshold diode micropulse photocoagulation for the treatment of clinically significant diabetic macular oedema. *Br J Ophthalmol.* 2005;89:74–80.
20. Luttrull JK, Musch DC, Spink CA. Subthreshold diode micropulse panretinal photocoagulation for proliferative diabetic retinopathy. *Eye (Lond).* 2008;22:607–612.
21. Luttrull JK, Spink CJ. Serial optical coherence tomography of subthreshold diode laser micropulse photocoagulation for diabetic macular edema. *Ophthalmic Surg Lasers Imaging.* 2006;37:370–377.
22. Ohkoshi K, Yamaguchi T. Subthreshold micropulse diode laser photocoagulation for diabetic macular edema in Japanese patients. *Am J Ophthalmol.* 2010;149:133–139.
23. Vujosevic S, Bottega E, Casciano M, Pilotto E, Convento E, Midena E. Microperimetry and fundus autofluorescence in diabetic macular edema: subthreshold micropulse diode laser versus modified early treatment diabetic retinopathy study laser photocoagulation. *Retina.* 2010;30:908–916.
24. Arjamaa O, Nikinmaa M. Oxygen-dependent diseases in the retina: role of hypoxia-inducible factors. *Exp Eye Res.* 2006;83:473–483.
25. Arjamaa O, Nikinmaa M, Salminen A, Kaarniranta K. Regulatory role of HIF-1alpha in the pathogenesis of age-related macular degeneration (AMD). *Ageing Res Rev.* 2009;8:349–358.
26. Klein R, Klein BE, Knudtson MD, Wong TY, Shankar A, Tsai MY. Systemic markers of inflammation, endothelial dysfunction, and age-related maculopathy. *Am J Ophthalmol.* 2005;140:35–44.
27. Beckham JT, Wilmink GJ, Mackanos MA, et al. Role of HSP70 in cellular thermotolerance. *Lasers Surg Med.* 2008;40:704–715.
28. Lanneau D, de Thonel A, Maurel S, Didelot C, Garrido C. Apoptosis versus cell differentiation: role of heat shock proteins HSP90, HSP70 and HSP27. *Prion.* 2007;1:53–60.
29. Rylander MN, Feng Y, Bass J, Diller KR. Thermally induced injury and heat-shock protein expression in cells and tissues. *Ann N Y Acad Sci.* 2005;1066:222–242.
30. Soti C, Nagy E, Giricz Z, Vigh L, Csermely P, Ferdinandy P. Heat shock proteins as emerging therapeutic targets. *Br J Pharmacol.* 2005;146:769–780.
31. Franklin TB, Krueger-Naug AM, Clarke DB, Arrigo AP, Currie RW. The role of heat shock proteins Hsp70 and Hsp27 in cellular protection of the central nervous system. *Int J Hyperthermia.* 2005;21:379–392.
32. Whitlock NA, Lindsey K, Agarwal N, Crosson CE, Ma JX. Heat shock protein 27 delays Ca2+-induced cell death in a caspase-dependent and -independent manner in rat retinal ganglion cells. *Invest Ophthalmol Vis Sci.* 2005;46:1085–1091.
33. Yenari MA, Liu J, Zheng Z, Vexler ZS, Lee JE, Giffard RG. Antiapoptotic and anti-inflammatory mechanisms of heat-shock protein protection. *Ann N Y Acad Sci.* 2005;1053:74–83.
34. Awasthi N, Wagner BJ. Upregulation of heat shock protein expression by proteasome inhibition: an antiapoptotic mechanism in the lens. *Invest Ophthalmol Vis Sci.* 2005;46:2082–2091.
35. Desmettre T, Maurage CA, Mordon S. Heat shock protein hyperexpression on chorioretinal layers after transpupillary thermotherapy. *Invest Ophthalmol Vis Sci.* 2001;42:2976–2980.
36. Desmettre T, Maurage CA, Mordon S. Transpupillary thermotherapy (TTT) with short duration laser exposures induce heat shock protein (HSP) hyperexpression on choroidoretinal layers. *Lasers Surg Med.* 2003;33:102–107.
37. Kim JM, Park KH, Kim YJ, Park HJ, Kim DM. Thermal injury induces heat shock protein in the optic nerve head in vivo. *Invest Ophthalmol Vis Sci.* 2006;47:4888–4894.
38. She H, Li X, Yu W. Subthreshold transpupillary thermotherapy of the retina and experimental choroidal neovascularization in a rat model. *Graefes Arch Clin Exp Ophthalmol.* 2006;244:1143–1151.
39. Beckham JT, Mackanos MA, Crooke C, et al. Assessment of cellular response to thermal laser injury through bioluminescence imaging of heat shock protein 70. *Photochem Photobiol.* 2004;79:76–85.
40. Kruse DE, Mackanos MA, O'Connell-Rodwell CE, Contag CH, Ferrara KW. Short-duration-focused ultrasound stimulation of Hsp70 expression in vivo. *Phys Med Biol.* 2008;53:3641–3660.
41. O'Connell-Rodwell CE, Mackanos MA, Simanovskii D, et al. In vivo analysis of heat-shock-protein-70 induction following pulsed laser irradiation in a transgenic reporter mouse. *J Biomed Opt.* 2008;13:30501.
42. O'Connell-Rodwell CE, Shriver D, Simanovskii DM, et al. A genetic reporter of thermal stress defines physiologic zones over a defined temperature range. *FASEB J.* 2004;18:264–271.
43. Blumenkranz MS, Yellachich D, Andersen DE, et al. Semiautomated patterned scanning laser for retinal photocoagulation. *Retina.* 2006;26:370–376.
44. Paulus YM, Jain A, Gariano RF, et al. Healing of retinal photocoagulation lesions. *Invest Ophthalmol Vis Sci.* 2008;49:5540–5545.
45. Belloc F, Dumain P, Boisseau MR, et al. A flow cytometric method using Hoechst 33342 and propidium iodide for simultaneous cell cycle analysis and apoptosis determination in unfixed cells. *Cytometry.* 1994;17:59–65.
46. Bevensee MO, Schwiening CJ, Boron WF. Use of BCECF and propidium iodide to assess membrane integrity of acutely isolated CA1 neurons from rat hippocampus. *J. Neurosci Methods.* 1995;58:61–75.
47. Wilde GJ, Sundström LE, Iannotti F. Propidium iodide in vivo: an early marker of neuronal damage in rat hippocampus. *Neurosci Lett.* 1994;180:223–226.
48. Unal Cevik I, Dalkara T. Intravenously administered propidium iodide labels necrotic cells in the intact mouse brain after injury. *Cell Death Differentiation.* 2003;10:928–929.
49. Yeh CJ, Hsi BL, Faulk WP. Propidium iodide as a nuclear marker in immunofluorescence. II. Use with cellular identification and viability studies. *J Immunol Methods.* 1981;43:269–275.
50. Rasband W. ImageJ [software]. Bethesda, MD: National Institutes of Health. Available at: http://rsb.info.nih.gov/ij/index.html. Accessed March 2010.
51. Wilmink GJ, Opalenik SR, Beckham JT, et al. In-vivo optical imaging of hsp70 expression to assess collateral tissue damage associated with infrared laser ablation of skin. *J Biomed Opt.* 2008;13:54066.
52. Sramek C, Paulus Y, Nomoto H, Huie P, Brown J, Palanker D. Dynamics of retinal photocoagulation and rupture. *J Biomed Opt.* 2009;14:34007.
53. COMSOL Multiphysics 3.5 [software]. COMSOL Inc. Available at: http://www.comsol.com/. Accessed March 2010.
54. Niemz M. *Laser-Tissue Interactions: Fundamentals and Applications*. Berlin: Springer; 2002.
55. Birngruber R, Hillenkamp F, Gabel VP. Theoretical investigations of laser thermal retinal injury. *Health Phys.* 1985;48:781–796.
56. Reich SJ, Fosnot J, Kuroki A, et al. Small interfering RNA (siRNA) targeting VEGF effectively inhibits ocular neovascularization in a mouse model. *Mol Vis.* 2003;9:210–216.
57. Tobe T, Ortega S, Luna JD, et al. Targeted disruption of the FGF2 gene does not prevent choroidal neovascularization in a murine model. *Am J Pathol.* 1998;153:1641–1646.
58. Wang H-C, Brown J, Alayon H, Stuck BE. Transplantation of quantum dot-labelled bone marrow-derived stem cells into the vitreous of mice with laser-induced retinal injury: survival, integration and differentiation. *Vis Res.* 2010;50:665–673.
59. Guo Y, Yao G, Lei B, Tan J. Monte Carlo model for studying the effects of melanin concentrations on retina light absorption. *Optics Image Sci Vis.* 2008;25:304–311.

60. Birngruber R. Choroidal circulation and heat convection at the fundus of the eye: implications for laser coagulation and the stabilization of retinal temperature. *Laser App Med Biol.* 1991;5:277–361.
61. Hammond BR Jr, Caruso-Avery M. Macular pigment optical density in a Southwestern sample. *Invest Ophthalmol Vis Sci.* 2000;41: 1492–1497.
62. Schule G, Huttmann G, Framme C, Roider J, Brinkmann R. Noninvasive optoacoustic temperature determination at the fundus of the eye during laser irradiation. *J Biomed Opt.* 2004;9:173–179.
63. Remtulla S, Hallett PE. A schematic eye for the mouse, and comparisons with the rat. *Vis Res.* 1985;25:21–31.
64. Algvere PV, Torstensson PA, Tengroth BM. Light transmittance of ocular media in living rabbit eyes. *Invest Ophthalmol Vis Sci.* 1993;34:349–354.
65. Birngruber R, Drechsel E, Hillenkamp F, Gabel V-P. Minimal spot size on the retina formed by the optical system of the eye. *Int Ophthalmol* 1979;1:175–178.
66. Kidwell TP, Priebe LA, Welch AJ. Measurement of ocular transmittance and irradiation distribution in argon-laser irradiated rabbit eyes. *Invest Ophthalmol.* 1976;15:668–671.
67. Schuele G, Rumohr M, Huettmann G, Brinkmann R. RPE damage thresholds and mechanisms for laser exposure in the microsecond-to-millisecond time regimen. *Invest Ophthalmol Vis Sci.* 2005;46: 714–719.
68. Banerjee RK, Zhu L, Gopalakrishnan P, Kazmierczak MJ. Influence of laser parameters on selective retinal treatment using single-phase heat transfer analyses. *Med Phys.* 2007;34:1828–1841.
69. Obana A. The therapeutic range of chorioretinal photocoagulation with diode and argon lasers: an experimental comparison. *Lasers Light Ophthalmol.* 1992;4:147–156.
70. Frankhauser F. Lasers, optical systems and safety in ophthalmology: a review. *Graefes Arch Clin Exp Ophthalmol.* 1996;234:473–487.
71. Hu CL, Barnes FS. The thermal-chemical damage in biological material under laser irradiation. *IEEE Trans Bio-med Eng.* 1970; 17:220–229.
72. Bhowmick S, Coad JE, Swanlund DJ, Bischof JC. In vitro thermal therapy of AT-1 Dunning prostate tumours. *Int J Hyperth.* 2004; 20:73–92.
73. Lepock JR. Cellular effects of hyperthermia: relevance to the minimum dose for thermal damage. *Int J Hyperth.* 2003;19:252–266.
74. Flanagan SW, Ryan AJ, Gisolfi CV, Moseley PL. Tissue-specific HSP70 response in animals undergoing heat stress. *Am J Physiol.* 1995;268:R28–32.
75. Rylander M, Diller K, Wang S, Aggarwal S. Correlation of HSP70 expression and cell viability following thermal stimulation of bovine aortic endothelial cells. *J Biomech Eng.* 2005;127:751–757.
76. Mainster MA, Reichel E. Transpupillary thermotherapy for age-related macular degeneration: long-pulse photocoagulation, apoptosis, and heat shock proteins. *Ophthalmic Surg Lasers.* 2000; 31:359–373.
77. Ibarra MS, Hsu J, Mirza N, et al. Retinal temperature increase during transpupillary thermotherapy: effects of pigmentation, subretinal blood, and choroidal blood flow. *Invest Ophthalmol Vis Sci.* 2004;45:3678–3682.
78. Sliney DH, Mellerio J, Gabel V-P, Schulmeister K. What is the meaning of threshold in laser injury experiments? Implications for human exposure limits. *Health Phys.* 2002;82:335–347.